Available online at www.sciencedirect.com
ScienceDirect
Ceramics International 35 (2009) 3269–3273
CERAMICS INTERNATIONAL
www.elsevier.com/locate/ceramint

Rapid fabrication of bulk graded Al_2O_3/YAG/YSZ eutectics by combustion synthesis under ultra-high-gravity field

Jun Pei [a,b,*], Jiang-Tao Li [a], Rui Liang [c], Ke-Xin Chen [c]

[a] Technical Institute of Physics and Chemistry, Chinese Academy of Sciences, Beijing 100080, China
[b] Graduate School of the Chinese Academy of Sciences, Beijing 100039, China
[c] Department of Materials Science and Engineering, Tsinghua University, Beijing 100084, China

Received 26 February 2009; received in revised form 18 March 2009; accepted 22 May 2009
Available online 18 June 2009

Abstract

A rapid and simple way of producing bulk graded Al_2O_3/YAG/YSZ ternary eutectics was investigated. The combustion reaction between Al/Fe_2O_3/Y_2O_3/ZrO_2 led to the formation of molten mixtures consisting of Al_2O_3/YAG/YSZ, and the subsequent separation of the ceramic melt from the iron melt was realized under ultra-high-gravity field, followed by the solidification of the ceramic melt. The as-solidified ceramic ingot sank into the iron melt, where an instantaneous isostatic pressure about 2 MPa was exerted on the around of the ceramic ingot resulting in an enhanced degree of densification. Microstructure analysis demonstrated that densified ceramic was composed of Al_2O_3/YAG/YSZ ternary eutectics. The phase composition, morphologies, hardness and fracture toughness of the eutectic product changed gradually along the direction of high gravity field. The maximum density of the eutectic ceramic was 97.32%, correspondingly, the maximum value of the Vickers hardness and fracture toughness reached 17.82 GPa and 5.51 MPa $m^{1/2}$, respectively.

Keywords: Eutectic ceramics; Combustion synthesis; Ultra-high-gravity; Melt

1. Introduction

The eutectic oxide ceramics fabricated by solidification from melts exhibit excellent high temperature mechanical properties, thermal stability and oxidation resistance. Therefore these eutectic oxide ceramics are potential candidates for elevated temperature structural application on turbine components [1–4]. Compared with the conventional sintered ceramics, the eutectic oxide ceramics prepared by solidification from melts offer important advantages for elevated temperature applications due to the unique characteristic microstructure feature with fine crystals entangled with each other and lots of clean interfaces [5]. However, the large-scale bulk ingot rather than fiber or rod could not be achieved easily due to the low thermal conductivity of the oxide ceramics. So, it seems to be inefficient and uneconomical to the traditional methods of fabricating eutectic oxide from melts [6–8].

From the functional graded material (FGM) of view, gradual changes in composition, microstructure and porosity result in gradients in properties such as mechanical strength and thermal conductivity and so on, therefore the materials with graded microstructure may offer great promise in wide applications [9].

In the present work we have developed a rapid and simple method of fabricating the eutectic oxide Al_2O_3/YAG/YSZ with graded structure. That is to integrate thermite reaction with ultra-high-gravity field. The high temperature molten mixture is obtained by the reaction of Al and Fe_2O_3 with additives of Y_2O_3 and ZrO_2 powders, meanwhile, the separation of the ceramic product melt from iron product melt completes in a short time in exerted ultra-high-gravity field. After that, the rapid solidification of Al_2O_3/YAG/YSZ melt is to be realized, accompanying the development of graded structure in ultra-high-gravity field.

2. Experiment

Commercial powders of Al (AR, Angang Group Aluminium Powder Co., Ltd., China), Fe_2O_3 (AR, Beijing Chemical Corporation, China), Y_2O_3 (99.999%, General Research Institute for Nonferrous Metals, China), and ZrO_2 (AR, Beijing

* Corresponding author at: Technical Institute of Physics and Chemistry, Chinese Academy of Sciences, Beijing 100080, China. Tel.: +86 10 82543693; fax: +86 10 82543693.
E-mail address: peijunipc@163.com (J. Pei).

0272-8842/$36.00.
doi:10.1016/j.ceramint.2009.05.019

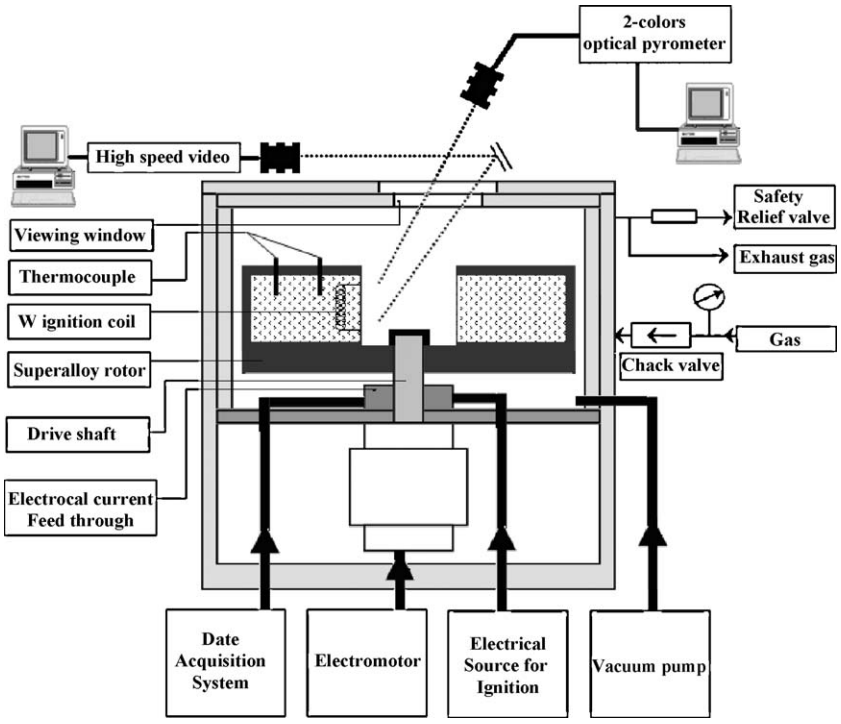

Fig. 1. Schematic diagram of the apparatus designed for carrying out the combustion synthesis under ultra-high-gravity.

Chemical Corporation, China) were used as starting materials. The raw materials were mixed according to the molar ratio of 17.7:52.3:11.8:18.2 and then homogenized by ball-milling in ethanol media for 2 h. The thermite reaction of the Al and Fe_2O_3 was shown as Eq. (1) [10]

$$2Al + Fe_2O_3 \rightarrow Al_2O_3 + 2Fe + 836\,kJ \quad (1)$$

The homogenized reactant powders were fully dried for 24 h and passed through a sieve of 100-mesh, and then the obtained powders were cold-pressed into a cylindrical graphite crucible with inner diameter of 30 mm (the weight was 200 g). The compact density of powder was controlled about 55% of the theoretical value. The crucible was mounted on a Ni-based super alloy rotor in an apparatus which was specially designed to carry out the combustion synthesis melt-casting under ultra-high-gravity (CSMC-UHG). The CSMC-UHG apparatus is schematically represented in Fig. 1. The experimental procedures were as follows: (a) started rotor to achieve an acceleration of about 1000 g at the end-edge of the sample, (b) ignited of mixture, (c) evacuated of the chamber down to 10^{-5} MPa to remove reaction gases, and (d) cooled of products. It was noted that the ceramic product was wrapped partly by the iron product. After separated from the iron, the bulk ceramic was cut into samples with a diamond saw, and the samples A, B, C, D, E and F were marked according to Fig. 2.

The crystallographic phase analysis was performed by X-ray diffraction (XRD, Rigaku, D/Max-IIB). The microstructure of the samples was observed by Scanning Electron Microscopy (SEM, HITACHIS-4300). The density of the samples was determined by the Archimedes method. A Vickers indentation equipment was used to measure the hardness and the fracture toughness with a load of 5 kg and applied time of 15 s, and the values of Vickers hardness and the fracture toughness were calculated by Eqs. (2) and (3) respectively [11,12]. The each mean value presented was obtained from five independent measurements in some area.

$$H_V = k_1 P/d^2 \quad (2)$$

$$K_{IC} = k_2 (E/H)^{1/2} (P/c^{3/2}) \quad (3)$$

where H_V is the Vickers hardness, K_{IC} is the fracture toughness, P is the indentation load, and d is the indentation diagonal, E is the Young's modulus of the material and obtained from nano-indentation test, c is the crack length, k_1 and k_2 are the dimensionless constants determined experimentally.

3. Results and discussion

Fig. 3 showed the relative density of samples from A to E. The relative densities of all samples were higher than 95.00%, and the maximum value reached 97.32%. Thus, the densifica-

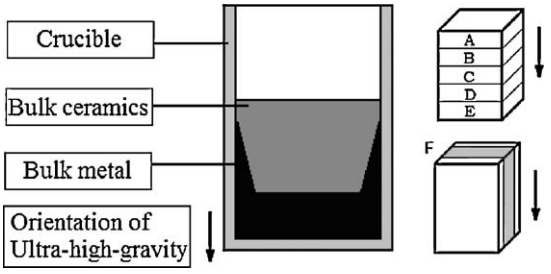

Fig. 2. Schematic diagram of the ceramics product assemblage by combustion synthesis under ultra-high-gravity and the manner of sampling the eutectic ceramic ingots.

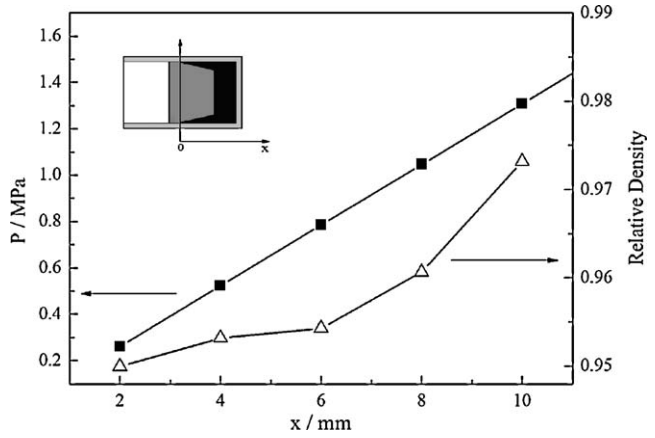

Fig. 3. Calculated value of equivalent pseudo-hot isostatic pressure and the measured relative density at function of sampling position.

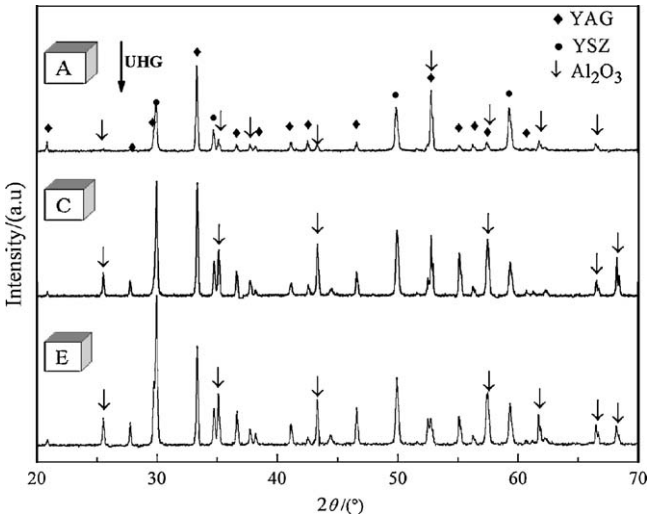

Fig. 4. X-ray diffraction patterns of A, C and E sampled perpendicular to the ultra-high-gravity.

tion of eutectic ceramic has been achieved by integrating combustion synthesis with ultra-high-gravity field.

Fig. 4 showed the X-ray diffraction spectra of samples A, C and E. It was found that each sample consisted of Al_2O_3, YAG ($Y_3Al_5O_{12}$), and YSZ (Y_2O_3 stabilized ZrO_2). The main peaks of alumina phase in sample A are apparently higher than that in samples C and E, which evidently indicates the gradient distribution of alumina phase in bulk Al_2O_3/YAG/YSZ eutectic product.

The gradient distribution of alumina could also be revealed by the microstructure features shown in Fig. 5(a–c), in which the dark area represented coarse alumina crystals with faceted interfaces, while the bright area represented ultra-fine eutectic microzone determined by EDS analysis. No pores and cracks existed in samples taken from top to bottom parallel to the direction of exerted ultra-high-gravity field. The coarse alumina crystals were well dispersed in an ultra-fine eutectic microzone with gradient distribution (Fig. 5c). The distribution histogram of coarse alumina is showed by Fig. 6, the size and quantity of the coarse alumina crystals increase from the sample (a to b), while decrease from (b to c).

Further observation of the ultra-fine eutectic micro-area mentioned above was performed by high magnified SEM (Fig. 5d–f) and EDS analysis. According to the EDS analysis, in the ultra-fine micro-area, the black zones were attributed to alumina, the gray zones to YAG and the fine white zones to ZrO_2. The phases of YAG and Al_2O_3 entangled with each other, and smaller ZrO_2 phase was widely dispersed in the interface between Al_2O_3 and YAG or in the phase of YAG.

As shown in Fig. 7, the hardness of the product increased and then decreased along the ultra-high-gravity field direction, while the dependence of fracture toughness on the distance was just opposite. This result was interestingly consistent with the graded distribution of alumina phases, as shown in Fig. 6. It indicated that the size and content of alumina crystals played an important role in controlling the mechanical properties of Al_2O_3/YAG/YSZ eutectic ceramics. The maximum value of Vickers hardness and the calculated fracture toughness reached 17.82 GPa and 5.51 MPa $m^{1/2}$, respectively. It must be mentioned that calculated fracture toughness according to the Eq. (3) was relatively accurate, therefore the calculated values here are only used as qualitative analysis to show the change law of the properties. The precisely direct analysis will be carried out and reported later.

The adiabatic temperature of the reaction Al and Fe_2O_3 was above 3600 K. When ultra-high-gravity field was introduced, the combustion velocity and temperature of thermite reaction would be further enhanced due to the speeding up heat and mass transmission [13]. Therefore, the products with the additives of Y_2O_3 and ZrO_2 would be in the state of melt because the thermite reaction could complete in a short time. In the melt mixture, YAG and Y stabilized ZrO_2 were developed. So, the iron melt (T_m = 1809 K), ceramic melt in the form of ternary eutectics (T_m = 1990 K) and pores were to be co-existing [6,14]. In the ultra-high-gravity field, the separation of these three phases should obey the Stock's law. Accordingly, the velocity of each phase could be calculated by Eq. (4)

$$v = \frac{2}{9}\frac{(\rho_1 - \rho_2)}{\eta} agr^2 \tag{4}$$

where v is the moving rate of the dispersed phase, r is the diameter of dispersed phase, a is the ultra-high-gravity magnitude, ρ_1 and ρ_2 represent the density of the dispersed phase and consecutive medium respectively, and η is the viscosity of the consecutive medium [15]. The moving rate of the dispersed phase depends on the $(\rho_1 - \rho_2)$, η, and a.

According to Eq. (4), in the present work, the separation velocity of iron (dispersed phase) from ceramic melt would be improved significantly to the higher level because of the viscosity decrease of ceramic melt. The calculated separation time of metal from ceramic melt was less than 5 s, which was in good agreement with the experimental result of the ceramic product without impurity of iron. The elimination time of residual pores from ceramic melt was less than 20 s, which would be further shortened by enhancing the level of ultra-high-gravity field. Hence, the fully densified Al_2O_3/YAG/YSZ eutectic ceramic would have been achieved by this technique.

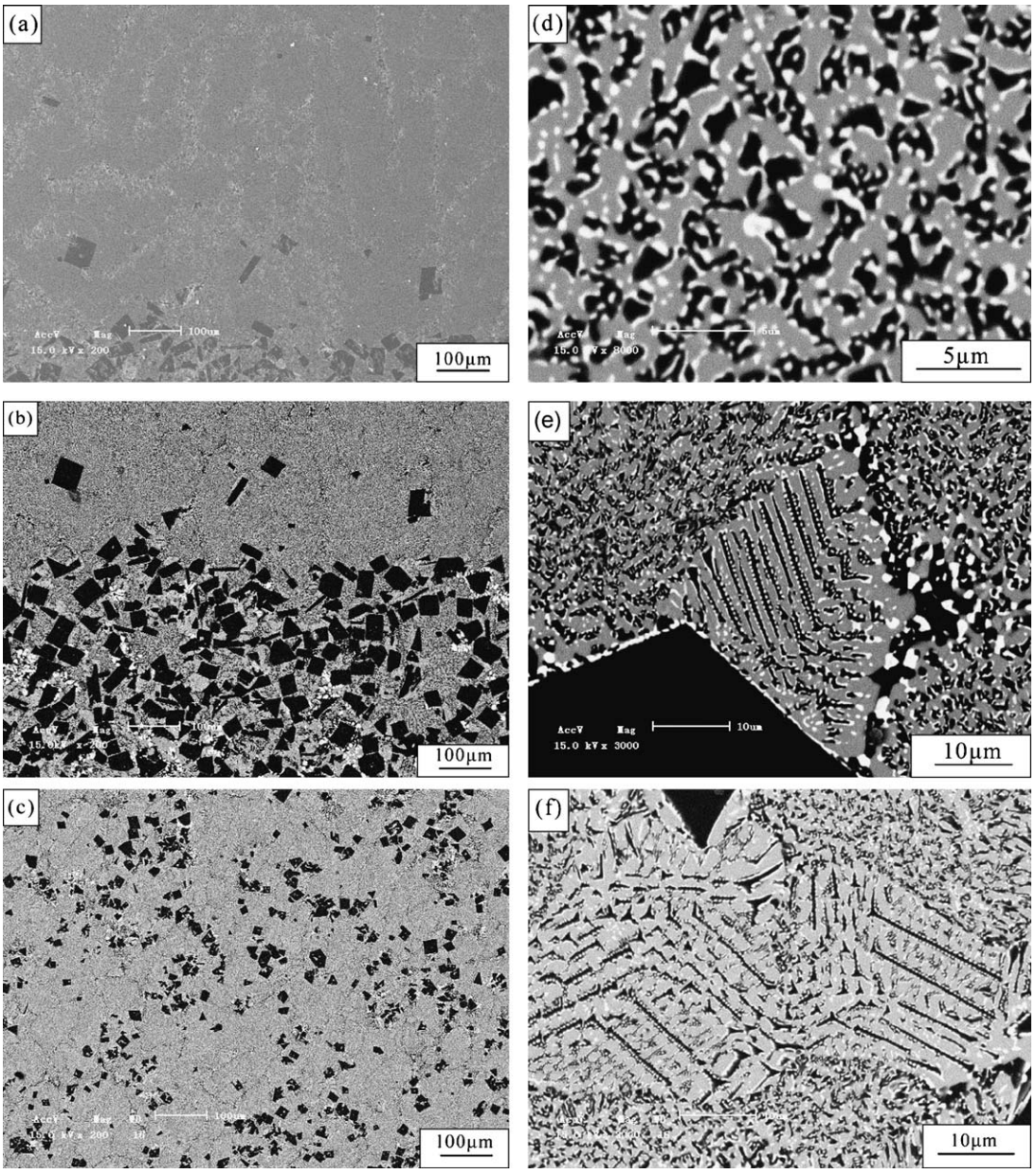

Fig. 5. SEM morphologies of different positions of the F sampled parallel to under ultra-high-gravity: (a–c) are the SEM pictures of top, middle and bottom respectively; (d–f) are magnified backscatter images corresponding to (a–c).

The as-precipitated crystal nucleus of alumina was driven toward the top of the crucible along opposite direction of UHG field, due to the different densities between alumina and molten mixture. With the increase of melt viscosity, when the motion-resistant force was beyond the buoyancy generated by ultra-high-gravity field, the alumina nucleus would stop moving and develop into grains. The grain size depended on the cooling rate of different areas. Therefore, the grains of the medium area

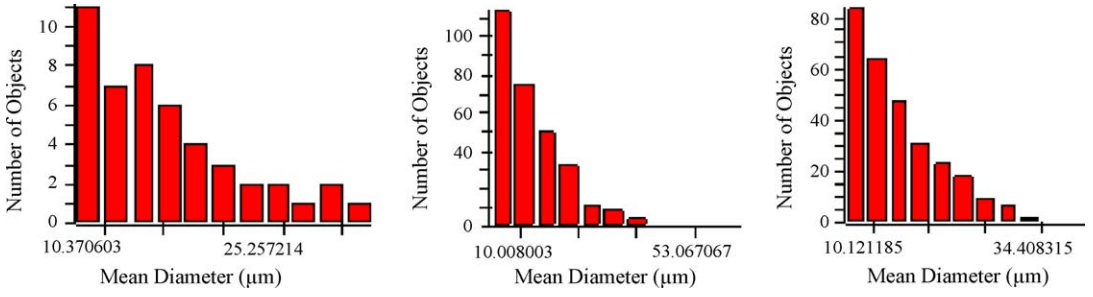

Fig. 6. Distribution histogram of Al_2O_3 grains size corresponding to the SEM morphologies of (a–c) in Fig. 5 measured by quantity image analysis.

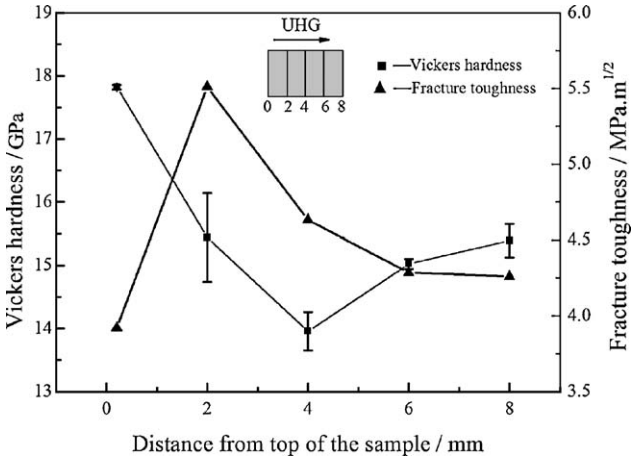

Fig. 7. Vickers hardness and fracture toughness of samples A–E.

grew larger than that of other areas because of the lowest cooling rate in the medium area.

Meanwhile, the eutectic melt was moved toward the bottom of the crucible along the ultra-high-gravity field direction. The viscosity of the margin eutectic melt increased more rapidly than that of the centre melt due to the difference of heat release rate. Therefore, the centre melt moved faster than the margin eutectic melt slightly, and a bulge of ceramic immerged into iron melt with different distance was developed along the ultra-high-gravity field direction. The eutectic melt was pressed to be densified by the surrounding iron melt, a transfer medium of pressure deriving from the high centrifugal force. So the densification of eutectic ceramic was remarkably enhanced by the iron melt. This process was properly described as pseudo-hot isostatic pressing, and the maximum pressure was estimated to be 2 MPa, as shown in Fig. 3.

4. Conclusions

Bulk densified Al_2O_3/YAG/YSZ ternary eutectic ceramics with graded structure was fabricated by combustion synthesis integrated with ultra-high-gravity. The formation, separation and densification of molten compounds consisting of Al_2O_3/YAG/YSZ and iron were realized under the ultra-high-gravity field in a short time. The as-solidified eutectic ceramic sank into the iron melt, where the density of the ceramic ingot was further enhanced by the instantaneous pseudo-hot isostatic pressing about 2 MPa. The phase composition, morphology, hardness and fracture toughness of the eutectic product changed gradually along the high gravity field direction. The maximum density of the eutectic ceramic was 97.32%, and correspondingly, the maximum value of the Vickers hardness and fracture toughness reached 17.82 GPa and 5.51 MPa $m^{1/2}$, respectively.

Acknowledgements

The financial support from both the National High-Tech and New Materials Projects under grant number 2006AA03Z112, and the National Natural Science Foundation under grant number 50772116 are gratefully acknowledged.

References

[1] Y. Waku, N. Nakagawa, T. Wakamoto, et al., A ductile ceramic eutectic composite with high strength at 1873 K, Nature. 389 (4) (1997) 49–52.
[2] Y. Mizutania, H. Yasuda, I. Ohnaka, et al., Coupled growth of unidirectionally solidified Al_2O_3–YAG eutectic ceramics, J. Cryst. Growth. 244 (2002) 384–392.
[3] J.M. Calderon-Moreno, M. Yoshimura, Al_2O_3–$Y_3Al_5O_{12}$ (YAG)–ZrO_2 ternary composite rapidly solidified from the eutectic melt, J. Euro. Ceram. Soc. 25 (2005) 1365–1368.
[4] Y. Harada, N. Uekawa, T. Kojima, et al., Formation of $Y_3Al_5O_{12}$–Al_2O_3 eutectic microstructure with off-eutectic composition, J. Euro. Ceram. Soc. 28 (2008) 1973–1978.
[5] T. Isobea, M. Omori, S. Uchidab, et al., Consolidation of Al_2O_3–$Y_3Al_5O_{12}$ (YAG) eutectic powder prepared from induction-melted solid and strength at high temperature, J. Euro. Ceram. Soc. 22 (2002) 2621–2625.
[6] J. LLorca, V.M. Orera, Directionally solidified eutectic ceramic oxides, Prog. Mater. Sci. 51 (2006) 711–809.
[7] B.M. Epelbaum, A. Yoshikawa, K. Shimamura, et al., Microstructure of Al_2O_3/$Y_3Al_5O_{12}$ eutectic fibers grown by μ-PD method, J. Cryst. Growth. 198/199 (1999) 471–475.
[8] H.J. Su, J. Zhang, C. Cui, et al., Rapid solidification of Al_2O_3/$Y_3Al_5O_{12}$/ZrO_2 eutectic in situ composites by laser zone remelting, J. Cryst. Growth. 307 (2007) 448–456.
[9] Y. Miyamoto, M. Niino, M. Koizumi, Functionally Graded Materials, Elsevier, The Netherlands, 1996, pp. 1–8.
[10] S. Yin, Combustion Synthesis (M), China Metallurgical Industry Press, 1999, p. 228.
[11] G.R. Anstis, P. Chantikul, B.R. Lawn, et al., A critical evaluation of indentation techniques for measuring fracture toughness: I, direct crack measurements, J. Am. Ceram. Soc. 64 (1981) 533–538.
[12] P. Chantikul, G.R. Anstis, B.R. Lawn, et al., A critical evaluation of indentation techniques for measuring fracture toughness: II, strength method, J. Am. Ceram. Soc. 64 (1981) 538–543.
[13] L.L. Wang, Z.A. Munir, Y.M. Maximov, Thermite reactions: their utilization in the synthesis and processing of materials, J. Mater. Sci. 28 (1993) 3693–3708.
[14] E.T. Turkdogan, Physical Chemistry of High Temperature Technology, Academic Press, 1980 (Chapter 3).
[15] R. Hinton, M. Dobrota, Density Gradient Centrifugation, North-Holland Biomedical Press, Holland, 1976 (Chapter 1).